Multi-ring signatures of the oscillation $\nu_\mu \to \nu_e$ in a water Cherenkov detector

A. Asratyan*, G.V. Davidenko, A.G. Dolgolenko, V.S. Kaftanov, M.A. Kubantsev†, and V. Verebryusov

Institute of Theoretical and Experimental Physics,

B. Cheremushkinskaya St. 25, Moscow 117259, Russia

February 7, 2008

Abstract

Multi-ring signatures of ν_e appearance via the oscillation $\nu_\mu \to \nu_e$ are formulated for a water Cherenkov detector. These signatures are appropriate for long-baseline neutrino experiments operating at relatively high neutrino energies $E_\nu > 2$ GeV that emphasize the matter effect. The NC background is less for selected multi-ring events than for 1e-like events, and may be directly estimated from the data. Sensitivity to the sign of Δm^2_{31} and to $\sin^2 2\theta_{13}$ is estimated for a conceptual scheme in which the proposed UNO detector is exposed to a neutrino beam from Fermilab's Main Injector. Also discussed is the physics potential of using a water Cherenkov detector in the NuMI program.

*Corresponding author. Tel.: + 7-095-237-0079; fax: + 7-095-127-0837; *E-mail address:* asratyan@vitep1.itep.ru.

†Now at Department of Physics and Astronomy, Northwestern University, Evanston, IL 60208, USA.

PACS: 14.60.Pq; 14.60.Fg

Keywords: Neutrino oscillations; ν_e appearance; Matter effect

Detecting the oscillation $\nu_\mu \to \nu_e$ in long-baseline accelerator experiments will provide clues to a number of neutrino-mixing parameters: the mixing angle θ_{13}, the sign of the "atmospheric" mass-squared difference Δm^2_{31}, and the CP-violating phase δ_{CP} [1]. The sign of Δm^2_{31} is correlated with that of the asymmetry between the $\nu_\mu \to \nu_e$ and $\bar{\nu}_\mu \to \bar{\nu}_e$ probabilities induced by the MSW matter effect [2, 3]; the magnitude of this asymmetry is roughly proportional to E_ν for neutrino energies well below the MSW resonance at some 10–15 GeV. At the same time, a similar asymmetry arising from CP violation only depends on the ratio L/E_ν. Therefore, the two effects can be disentangled by comparing the data for different baselines and energies. In the experiment JHF2K [4] due to start operation by the end of the decade, Super-Kamiokande will be irradiated by a ν_μ beam with $\langle E_\nu \rangle \simeq 0.7 - 0.8$ GeV over a baseline of $L = 295$ km. Likewise, in this paper we discuss using a water Cherenkov detector that offers good e/μ and e/h separation and spectrometry for electrons [5], but assume substantially bigger energy and baseline so as to emphasize the matter effect compared to JHF2K.

To be specific, we assume that the medium-energy beam[1] of Fermilab's Main Injector is aimed at either of the three candidate sites for UNO—the proposed big water Cherenkov detector with fiducial mass of $\sim$ 500 kilotons [7]. These sites include the Homestake mine in Lead, South Dakota ($L = 1280$ km); the WIPP facility in Carlsbad, New Mexico ($L = 1770$ km); and the San Jacinto mountain in California ($L = 2620$ km). For comparison, we also consider a shorter baseline of $L = 900$ km, that is near the maximum value of L allowed by the original beamline of the NuMI–MINOS program [6] for far sites within 10 km of the beam axis [8].

[1]This is taken as the PH2me beam with peak energy of ν_μ flux near 6 GeV at zero angle, as designed for the NuMI–MINOS program [6].

Except for the longest baseline of $L = 2620$ km, we adopt the concept of an "off-axis" neutrino beam [9] that allows to enhance the ν_μ flux at oscillation maximum, as well as to suppress the backgrounds to $\nu_\mu \to \nu_e$ arising from NC collisions and from the ν_e component of the original beam. The off-axis angle θ_ν is selected so as to place the maximum of the E_ν distribution near the first maximum of the oscillation for $|\Delta m^2_{31}| \simeq 0.003$ eV^2: $\theta_\nu = 11.1$, 7.7, 5.6, and 0 mrad [10] for $L = 900$, 1280, 1770, and 2620 km, respectively. Figure 1 shows the oscillation-free E_ν spectra of all ν_μ- and ν_e-induced CC events for either site, assuming 4×10^{20} protons on target per year [6] and an exposure of 500 kton–years.

Our foremost task is to formulate the selections of ν_e-induced CC events appropriate for $E_\nu > 2$ GeV, so for simplicity the "solar" mass-squared difference Δm^2_{21} is set to zero thus excluding from the simulation any effects of intrinsic CP violation. The matter effect is estimated in the approximation of uniform matter density along the neutrino path [3], assuming $\rho = 3$ g/cm^3 for all baselines considered. Relevant neutrino-mixing parameters are assigned the values consistent with the atmospheric and reactor data [11, 12]: $\Delta m^2_{31} = \pm 0.003$ eV^2, $\sin^2 2\theta_{23} = 1$, and $\sin^2 2\theta_{13} = 0.1$ (the latter value is at the upper limit imposed in [12]). The simulation relies on the neutrino-event generator NEUGEN based on the Soudan-2 Monte Carlo [13], that takes full account of exclusive channels like quasielastics and excitation of baryon resonances.

At neutrino energies below 1 GeV, ν_e appearance can be efficiently detected by selecting 1-ring e-like events of the reaction $\nu_e N \to e^- X$ that is dominated by quasielastics. (Here and in what follows, X denotes a system of hadrons other than the π^0, in which the momenta of all charged particles are below the Cherenkov threshold in water.) The background largely comes from the flavor-blind NC reaction $\nu N \to \nu \pi^0 X$ whose cross section relative to $\nu_e N \to e^- X$ increases with E_ν, see Fig. 2. At low neutrino energies ~ 1 GeV, this NC reaction is suppressed by limited phase space and, moreover, the bulk of π^0 mesons are identified by resolving the rings of

two photons from $\pi^0 \to \gamma\gamma$ [2]. As a result, in JHF2K the $\nu N \to \nu\pi^0 N$ background is not expected to exceed the "intrinsic" ν_eCC background due to the original ν_e component of the beam [4]. The ν_τCC background, arising from the dominant oscillation $\nu_\mu \to \nu_\tau$ followed by $\nu_\tau N \to \tau^- X$ and $\tau^- \to e^-\nu\bar{\nu}$, is negligibly small due to the threshold effect in τ production. At higher neutrino energies discussed in this paper, the NC reaction $\nu N \to \nu\pi^0 X$ emerges as the dominant source of 1-ring e-like events, and the ν_τCC background tends to exceed the intrinsic ν_eCC background. This is illustrated by the upper panels in Figs. 3–6 where $E_{\rm vis}$ distributions of 1e-like events are shown for each baseline and either sign of Δm^2_{31}. (Depending on the reaction, $E_{\rm vis}$ stands for either the e^- or π^0 energy.) These distributions also illustrate the dependence of matter effect on neutrino energy.

As expected, the 1e-like signature of ν_e appearance proves to be less rewarding for $E_\nu > 2$ GeV than for $E_\nu < 1$ GeV. In this paper, we propose to detect the oscillation $\nu_\mu \to \nu_e$ by selecting 2- and 3-ring signatures of the reactions $\nu_e N \to e^-\pi^+ X$ and $\nu_e N \to e^-\pi^0 X$ that involve emission of a charged or neutral pion[3]. The motivation is that, at neutrino energies of a few GeV, the cross section for formation of $\Delta(1232)$ states alone is comparable to quasielastics, whereas the background final states $\nu\pi^0\pi N$ are suppressed with respect to $\nu\pi^0 N$. In other words, one may expect that demanding an extra pion in the final state will effectively reduce the NC background rather than the CC signal. This is illustrated by Fig. 2 showing the cross sections of relevant CC and NC reactions relative to $\nu_e N \to e^- X$ as functions of neutrino energy. The ratios between the cross sections of corresponding CC and NC reactions, $\sigma(\nu_e N \to e^-\pi^+ X)/\sigma(\nu N \to \nu\pi^0\pi^\pm X)$ and $\sigma(\nu_e N \to e^-\pi^0 X)/\sigma(\nu N \to \nu\pi^0\pi^0 X)$, are seen to be substantially larger than the ratio $\sigma(\nu_e N \to e^- X)/\sigma(\nu N \to \nu\pi^0 X)$.

The reaction $\nu_e N \to e^-\pi^+ X$ will produce two rings in the detector, of which

[2]The efficiency of π^0 reconstruction, as measured in the near detector of the K2K experiment [14], steeply decreases with increasing π^0 momentum and vanishes at $p(\pi^0) \simeq 900$ MeV [15].

[3]Here and below, corresponding antineutrino reactions are implicitly included.

one is e-like and the other is non-showering. Apart from the reaction $\nu N \to \nu\pi^0\pi^\pm X$ with two pions in the final state, a potentially dangerous source of NC background is the more frequent process $\nu p \to \nu\pi^0 p$ in which the momentum of the final proton is above the Cherenkov threshold. Note however that νN kinematics restrict the emission angles of such protons to the region $\cos\theta > 0.45$, whereas pions with momenta above the Cherenkov threshold may even travel in the backward hemisphere. A lower cut on emission angle of the non-showering particle, $\theta > 50^0$, rejects the bulk of visible protons from $\nu p \to \nu\pi^0 p$ and keeps nearly a half of visible pions emitted in the reaction $\nu_e N \to e^-\pi^+ X$. The latter cut will also prevent the π^+ ring from collapsing into the e^- ring. Therefore, we select 2-ring events featuring a e-like ring and an additional ring due to a non-showering particle with a large emission angle of $\theta > 50^0$. This is referred to as the $e\pi$ signature in Table 1 below. The distributions of thus selected events in visible energy $E_{\rm vis}$, defined as the energy of the e-like ring, are shown in the middle panels of Figs. 3–6 for $L = 900$, 1280, 1770, and 2620 km assuming incident neutrinos. The NC background is seen to be less for the selected $e\pi$-like events than for 1e-like events (compare with the top panels of the same Figures). That the ν_τCC background is also less for $e\pi$-like events than for quasielastics is due to a stronger threshold suppression of $\nu_\tau N \to \tau^-\pi^+ N$ compared to $\nu_\tau n \to \tau^- p$. On the other hand, the ν_μCC background is negligibly small for 1e-like events, but contributes to selected $e\pi$-like events through the reaction $\nu_\mu N \to \mu^-\pi^0 X$ in which the muon is emitted at a broad angle.

Next, we consider the reaction $\nu_e N \to e^-\pi^0 X$ that features a neutral pion in the final state[4]. Depending on whether or not the π^0 has been reconstructed, the observable signature is either three e-like rings of which two fit to $\pi^0 \to \gamma\gamma$, or two e-like rings that would not fit to a π^0. The NC background arises from the reaction $\nu N \to \nu\pi^0\pi^0 N$ in which at least one of the two π^0 mesons has not been reconstructed. Note that in the latter reaction the two π^0 mesons are emitted

[4] The first observation in a water Cherenkov detector of the corresponding ν_μ-induced reaction, $\nu_\mu N \to \mu^-\pi^0 X$, has been reported in [16].

with comparable energies, whereas in $\nu_e N \to e^- \pi^0 X$ the e^- tends to be the leading particle. This suggests a selection based on the absolute value of asymmetry $A = (E_1 - E_2)/(E_1 + E_2)$, where E_1 and E_2 are the energies of the two showers for the two-ring signature, and of the reconstructed π^0 and the "odd" shower—for the three-ring signature. The selection $|A| > 0.6$ has been adopted in this paper. The distributions of events featuring 2 or 3 e-like rings in visible energy $E_{\rm vis}$, defined as the total energy of all such rings, are shown in the bottom panels of Figs. 3–6 for incident neutrinos. Again, the NC and ν_τCC backgrounds are seen to be less than for 1e-like events.

The total number of $\nu_\mu \to \nu_e$ events is listed in Table 1 for either sign of Δm^2_{31}, signature, baseline, and beam setting, assuming an exposure of 500 kton-years. Note that for $\Delta m^2_{31} > 0$ (< 0) and incident (anti)neutrinos, the $e\pi$ and multi-e signals of $\nu_\mu \to \nu_e$ are virtually independent of the baseline despite the depletion of neutrino flux with distance. This is a combined effect of matter-induced enhancement, E_ν-dependence of one-pion production (see Fig. 2), and θ_ν-dependence of neutrino flux (see Fig. 1). We estimate the significance of $\nu_\mu \to \nu_e$ signals for the 1e, $e\pi$, and multi-e signatures in the approximation of zero systematic uncertainty on the background. The signal interval of $E_{\rm vis}$ is selected so as to maximize the quantity $F = S/\sqrt{B}$, where S and B are the numbers of signal and background events falling within the interval. Thus obtained values of F are also listed in Table 1.

The NC and ν_τCC backgrounds are dominant sources of systematics, and therefore we do not include the 1e-like events in our estimates of statistical significance of the $\nu_\mu \to \nu_e$ signal. Assuming $\Delta m^2_{31} > 0$ and incident neutrinos, for the combined sample of $e\pi$-like and multi-e-like events we obtain $F = 52.8$, 57.4, 52.7, and 48.5 for $L = 900$, 1280, 1770, and 2620 km, respectively. (Note that the significance of the $\nu_\mu \to \nu_e$ signal, like its magnitude, is fairly independent of the baseline.) Thus at 90% C.L., a one-year exposure of UNO in the ν beam will allow to probe the value of $\sin^2 2\theta_{13}$ down to 0.0022–0.0026 (depending on the baseline). Assuming

L, θ_ν	Signature	Total signal, ν beam	Total signal, $\bar{\nu}$ beam	F value, ν beam	F value, $\bar{\nu}$ beam
900 km, 11.1 mrad	$1e$	575 (330)	195(335)	41.6 (25.1)	23.8 (39.9)
	$e\pi$	400 (234)	87 (146)	43.4 (25.4)	17.4 (29.3)
	multi-e	152 (90)	35 (57)	30.4 (18.2)	11.3 (19.1)
1280 km, 7.7 mrad	$1e$	494 (207)	140 (328)	34.8 (15.9)	16.7 (36.8)
	$e\pi$	414 (179)	74 (167)	47.7 (21.1)	14.9 (33.1)
	multi-e	184 (81)	40 (86)	32.1 (14.7)	10.4 (22.8)
1770 km, 5.6 mrad	$1e$	383 (100)	72 (273)	27.9 (8.0)	8.6 (30.3)
	$e\pi$	358 (96)	42 (153)	43.8 (12.1)	8.4 (30.2)
	multi-e	174 (48)	27 (94)	29.5 (8.4)	6.7 (23.1)
2620 km, 0.0 mrad	$1e$	345 (54)	40 (267)	23.3 (3.7)	4.2 (25.5)
	$e\pi$	372 (57)	26 (172)	39.8 (6.7)	4.8 (27.8)
	multi-e	199 (29)	20 (130)	27.8 (4.6)	4.4 (24.1)

Table 1: Total number of $\nu_\mu \to \nu_e$ events and the "figure of merit" $F = S/\sqrt{B}$ for either sign of Δm^2_{31}, signature, baseline, and beam setting, assuming 4×10^{20} protons per year and an exposure of 500 kton–years. The first (second) value corresponds to the positive (negative) sign of the mass-squared difference Δm^2_{31}.

$\Delta m^2_{31} < 0$, after a one-year exposure of UNO in the $\bar{\nu}$ beam the experiment will be sensitive to $\sin^2 2\theta_{13}$ values down to 0.0032–0.0034. As soon as the number of delivered protons is increased from 4×10^{20} to 1.6×10^{21} per year, as envisaged in [17], values of $\sin^2 2\theta_{13}$ well below 10^{-3} will become accessible in a few years of data taking with the UNO detector at either of the three candidate sites. The reach in $\sin^2 2\theta_{13}$ will thus be comparable to that of the second phase of JHF2K based on Hyper-Kamiokande [4], but higher neutrino energy than in the latter experiment will also allow to probe the sign of Δm^2_{31}. Indeed, switching the sign of Δm^2_{31} effectively changes the ratio between the ν and $\bar{\nu}$ signals by a large factor of some 5, 14, and 43 for $L = 1280$, 1770, and 2620 km, respectively.

A far site corresponding to $L = 900$ km and $\theta_\nu = 11.1$ mrad is available with the original beamline of the NuMI program [8], and one may assume that a water Cherenkov detector with fiducial mass of 100 kt is built there. We estimate that in 5

years of operation with the ν ($\bar{\nu}$) beam, this experiment will be sensitive to $\sin^2 2\theta_{13}$ values down to 0.0024 (0.0036) for $\Delta m^2_{31} > 0$ ($\Delta m^2_{31} < 0$). Thus, the sensitivity to $\sin^2 2\theta_{13}$ will be better than in the first phase of the JHF2K experiment [4].

Note that unlike the $1e$ signature, the $e\pi$ and multi-e signatures may allow to estimate the NC background from the data: constraining the axes of all rings to a common point in space will yield the position of the primary vertex. Within errors, this should coincide with the reconstructed vertex of a e^--induced shower, whereas the vertex of an unresolved π^0 shower will be displaced along the shower direction by $\sim \lambda_\gamma$. Here, $\lambda_\gamma \simeq 55$ cm is the mean free path for photons in water. This has to be compared with spatial resolution for the vertex of a single e-like ring, estimated as 34 cm for Super-Kamiokande [5]. Therefore, provided that spatial resolution of UNO is sufficiently high, it may prove possible to directly estimate the NC background by analyzing the displacement of shower vertices from the reconstructed vertex of neutrino collision.

To conclude, we have formulated multi-ring signatures of the oscillation $\nu_\mu \to \nu_e$ in a water Cherenkov detector, that are appropriate for long-baseline neutrino experiments operating at relatively high neutrino energies $E_\nu > 2$ GeV. These emphasize the MSW matter effect and, therefore, may allow to determine the sign of the "atmospheric" mass-squared difference Δm^2_{31}. The NC background is less for selected multi-ring events than for $1e$-like events, and may be directly estimated from the data. Sensitivity to the sign of Δm^2_{31} and to $\sin^2 2\theta_{13}$ has been estimated for a conceptual scheme in which the proposed large water Cherenkov detector, UNO, is irradiated by a neutrino beam from Fermilab's Main Injector over a baseline of either 1280, 1770, or 2620 km. Compared to the second phase of the JHF–Kamioka experiment, the proposed scheme may show similar sensitivity to $\sin^2 2\theta_{13}$ and superior sensitivity to the sign of Δm^2_{31}. We have also discussed the physics potential of using a a water Cherenkov detector in the NuMI program.

References

[1] L. Wolfenstein, *Lepton physics and CP violation,* Proc. 9th Int. Workshop on Neutrino Telescopes, edited by M. Baldo Ceolin, Venice, March 2001, p. 35; H. Minakata and H. Nunokawa, JHEP 10, 001 (2001); M. Lindner, *The physics potential of future long-baseline neutrino oscillation experiments,* talk presented at the XXth Int. Conf. on Neutrino Physics and Astrophysics, Munchen, May 2002, TUM-HEP-474/02 (arXiv:hep-ph/0209083).

[2] L. Wolfenstein, Phys. Rev. D17, 2369 (1978); S. Mikheyev and A. Smirnov, Sov. J. Nucl. Phys. 42, 913 (1985).

[3] V. Barger, S. Geer, R. Raja, and K. Whisnant, Phys. Rev. D62, 013004 (2000); I. Mocioiu and R. Shrock, Phys. Rev. D62, 053017 (2000); M. Freund et al., Nucl. Instr. Meth. A451, 18 (2000).

[4] Y. Itow et al., *The JHF–Kamioka neutrino project,* KEK Report 2001-4, ICRR Report 477-2001-7, TRIUMF Report TRI-PP-01-05, June 2001 (see arXiv:hep-ex/0106019); R.R. Volkas, *Implications of the JHF–Kamioka neutrino oscillation experiment,* Proc. Workshop on Physics at the Japan Hadron Facility (World Scientific, Signapore, 2002), p. 73 (see arXiv:hep-ph/0211307).

[5] M. Shiozawa, in Proc. of RICH-98, Nucl. Instr. Meth. A433, 240 (1999).

[6] S. Wojcicki, Nucl. Phys. Proc. Suppl. 91, 91, 216 (2001); V. Paolone, Nucl. Phys. Proc. Suppl. 100, 197 (2001); M. Diwan, *Status of the MINOS experiment,* Invited talk presented at the 7th Int. Workshop on Tau Lepton Physics, Santa Cruz, September 2002 (arXiv:hep-ex/0211026); *Neutrino Oscillation Physics at Fermilab: the NuMI–MINOS Project,* Fermilab report NuMI-L-375, May 1998 (see http://www.hep.anl.gov/ndk/hypertext/numi_notes.html).

[7] C.K. Jung, *Feasibility of a next-generation underground water Cherenkov detector: UNO,* Proc. Workshop on Next Generation Nucleon Decay

and Neutrino Detector (NNN99), September 1999, Stony Brook, New York (see arXiv:hep-ex/0005046); M. Goodman et al. (UNO Proto-Collaboration), *Physics potential and feasibility of UNO,* June 2001 (see http://superk.physics.sunysb.edu/).

[8] A. Para and M. Szleper, *Neutrino oscillation experiments using off-axis NuMI beams,* Fermilab-PUB-01-324 (2001); S.E. Kopp, *The NuMI neutrino beam and potential for an off-axis experiment,* talk presented at the NuFact'02 Workshop, Imperial College, London, 2002 (arXiv:hep-ex/0210009); D. Ayres et al., *Letter of Intent to build an off-axis detector to study $\nu_\mu \rightarrow \nu_e$ oscillations with the NuMI neutrino beam,* Fermilab, July 17, 2002 (arXiv:hep-ex/0210005).

[9] D. Beavis et al., *Long-baseline neutrino oscillation experiment E889, physics design report,* BNL-52459, April 1995.

[10] The ν_μ and ν_e fluxes for these and other off-axis angles may be found at http://www-numi.fnal.gov/fnal_minos/new_initiatives/.

[11] Y. Fukuda et al. (Super-Kamiokande Coll.), Phys. Rev. Lett. 81, 1562 (1998); T. Kajita and Y. Totsuka, Rev. Mod. Phys. 73, 85 (2001); M. Shiozawa (for the Super-Kamiokande Coll.), talk presented at the XXth Int. Conf. on Neutrino Physics and Astrophysics, Munchen, May 2002.

[12] M. Apollonio et al. (CHOOZ Coll.), Phys. Lett. B466, 415 (1999).

[13] H. Gallagher, *The NEUGEN neutrino event generator,* talk presented at the NuInt01 Workshop, KEK, Dec. 2001 (see http://neutrino.kek.jp/nuint01/); H. Gallagher and M. Goodman, *Neutrino Cross Sections,* Fermilab report NuMI-112, PDK-626, November 1995 (see http://www.hep.anl.gov/ndk/hypertext/numi_notes.html).

[14] S.H. Ahn et al. (K2K Coll.), Phys. Lett. B511, 178 (2001); T. Ishii, *New results from K2K,* arXiv:hep-ex/0206033.

[15] C. Mauger, *Neutral current π^0 production in K2K and SuperK water Cherenkov detectors,* talk presented at the NuInt01 Workshop, KEK, Dec. 2001 (see http://neutrino.kek.jp/nuint01/).

[16] S. Mine, *Study of ν backgrounds to nucleon decay using K2K 1KT detector data,* talk presented at the NuInt01 Workshop, KEK, Dec. 2001 (see http://neutrino.kek.jp/nuint01/).

[17] W. Chou and B. Foster (eds.), *Proton Driver Design Study,* Fermilab-TM-2136 (2000) and Fermilab-TM-2169 (2002) (see http://projects.fnal.gov/protondriver/).

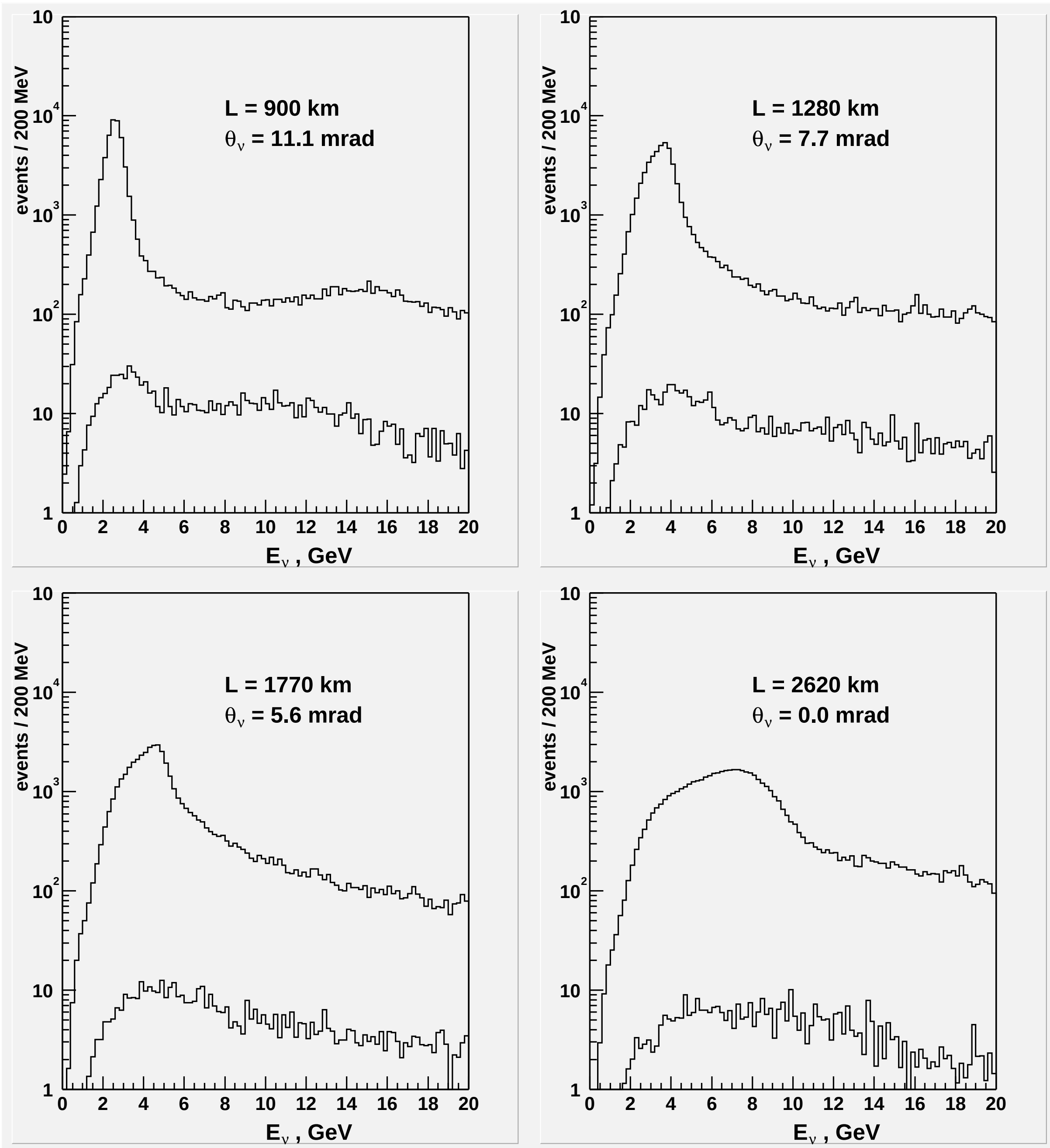

Figure 1: The oscillation-free E_ν spectra of ν_μ- and ν_e-induced CC events (upper and lower histograms, respectively) for four locations in the medium-energy beam of Fermilab's Main Injector: $L = 900$ km and $\theta_\nu = 11.1$ mrad (top left), $L = 1280$ km and $\theta_\nu = 7.7$ mrad (top right), $L = 1770$ km and $\theta_\nu = 5.6$ mrad (bottom left), and $L = 2620$ km and $\theta_\nu = 0$ mrad (bottom right). For incident neutrinos and an exposure of 500 kton-years.

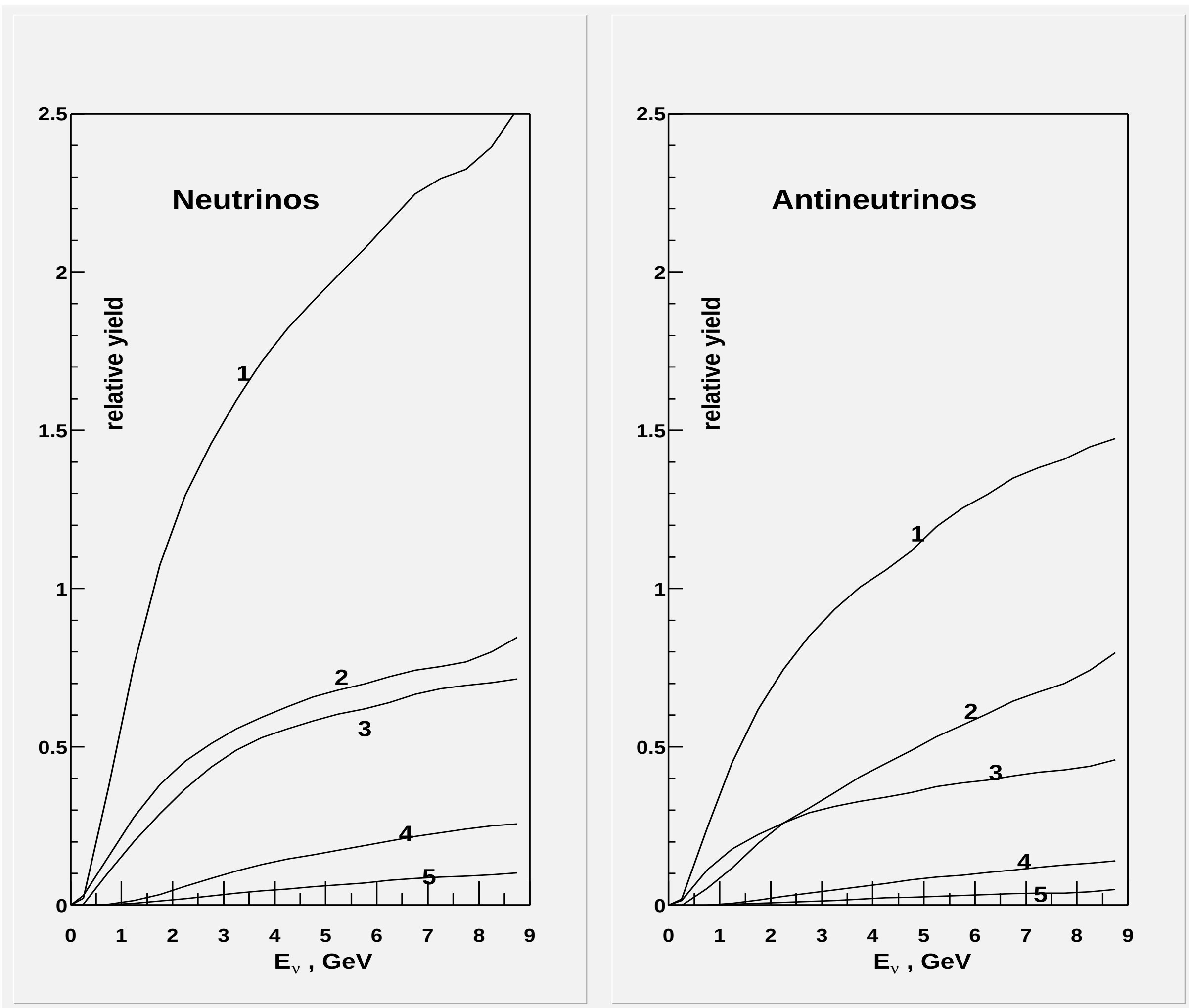

Figure 2: Cross sections per mean nucleon in water of relevant CC and NC reactions, divided by the $\nu_e N \to e^- X$ cross section, as functions of neutrino energy: $\nu_e N \to e^- \pi^+ X$ (curve 1), $\nu_e N \to e^- \pi^0 X$ (curve 2), $\nu N \to \nu \pi^0 X$ (curve 3), $\nu N \to \nu \pi^0 \pi^\pm X$ (curve 4), and $\nu N \to \nu \pi^0 \pi^0 X$ (curve 5). The left- and right-hand panels are for incident neutrinos and antineutrinos, respectively.

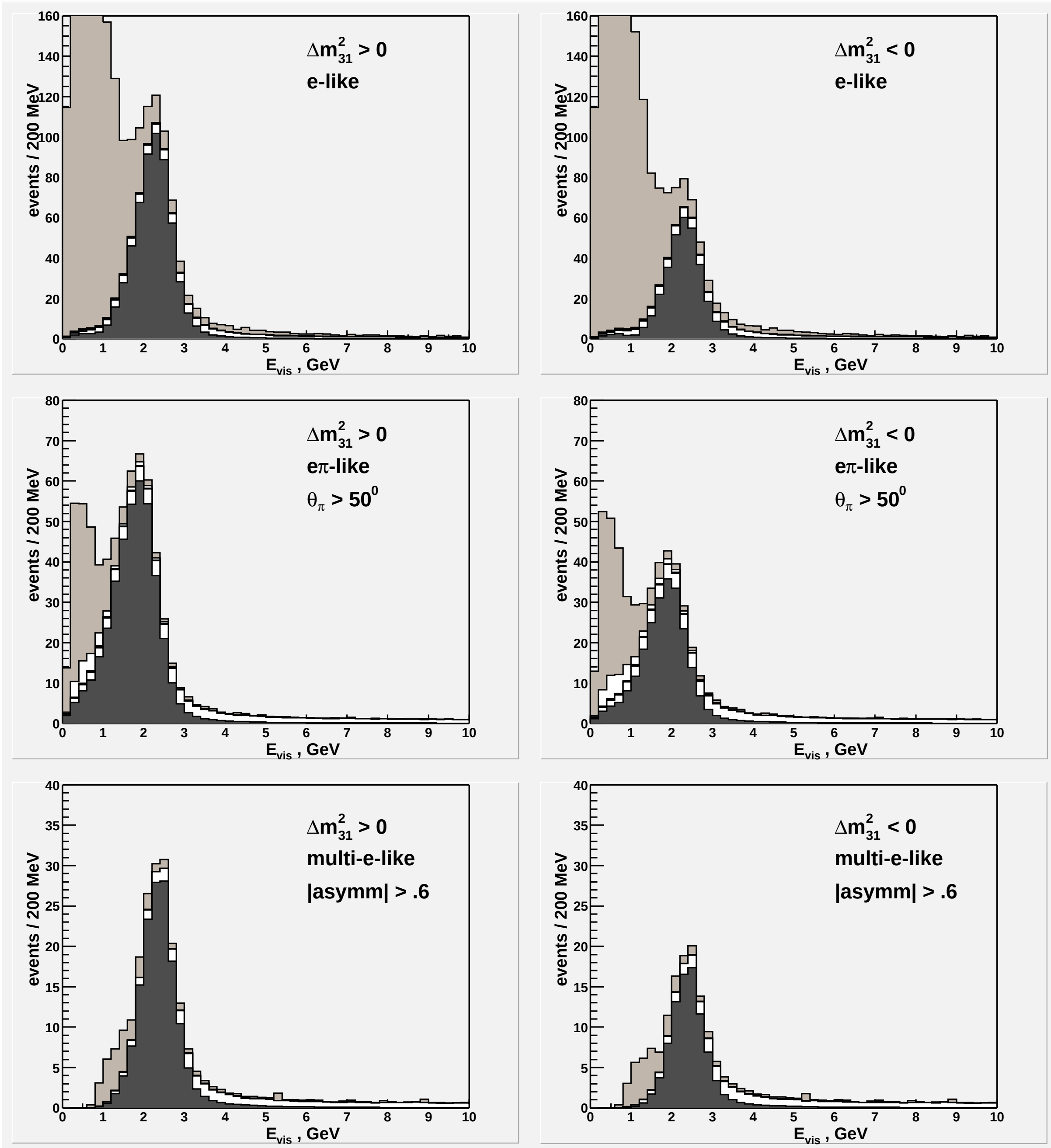

Figure 3: For $L = 900$ km, $\theta_\nu = 11.1$ mrad, and incident neutrinos, $E_{\rm vis}$ distributions of 1e-like events (top panels), $e\pi$-like events (middle panels), and multi-e-like events (bottom panels). The left- and right-hand panels are for $\Delta m^2_{31} > 0$ and $\Delta m^2_{31} < 0$, respectively. From bottom, the depicted components are the $\nu_\mu \to \nu_e$ signal (shaded area), intrinsic ν_eCC background (white area), ν_τCC background (black area), ν_μCC background (white area), and the NC background (light-shaded area).

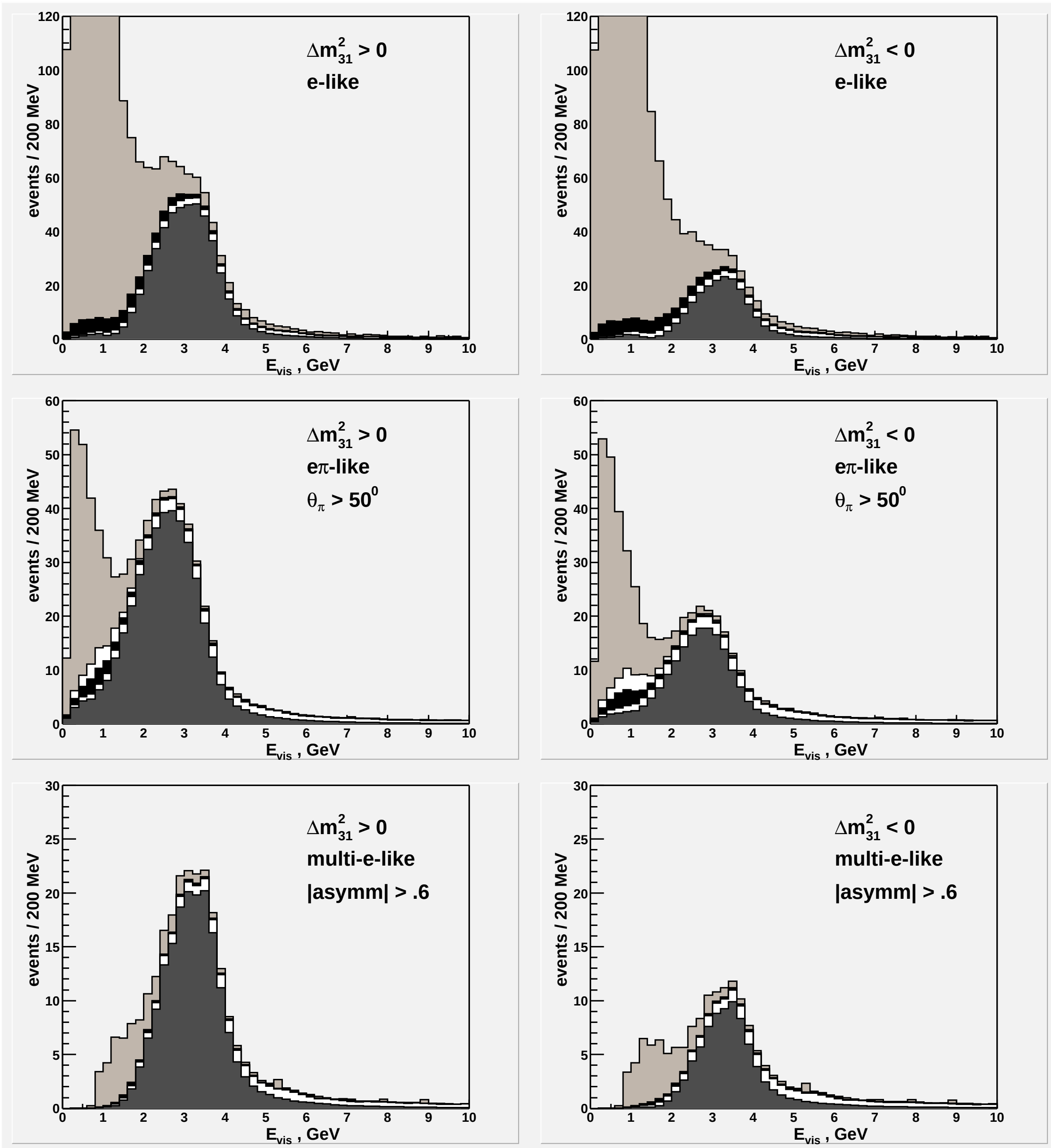

Figure 4: Same as Fig. 3, but for $L = 1280$ km and $\theta_\nu = 7.7$ mrad.

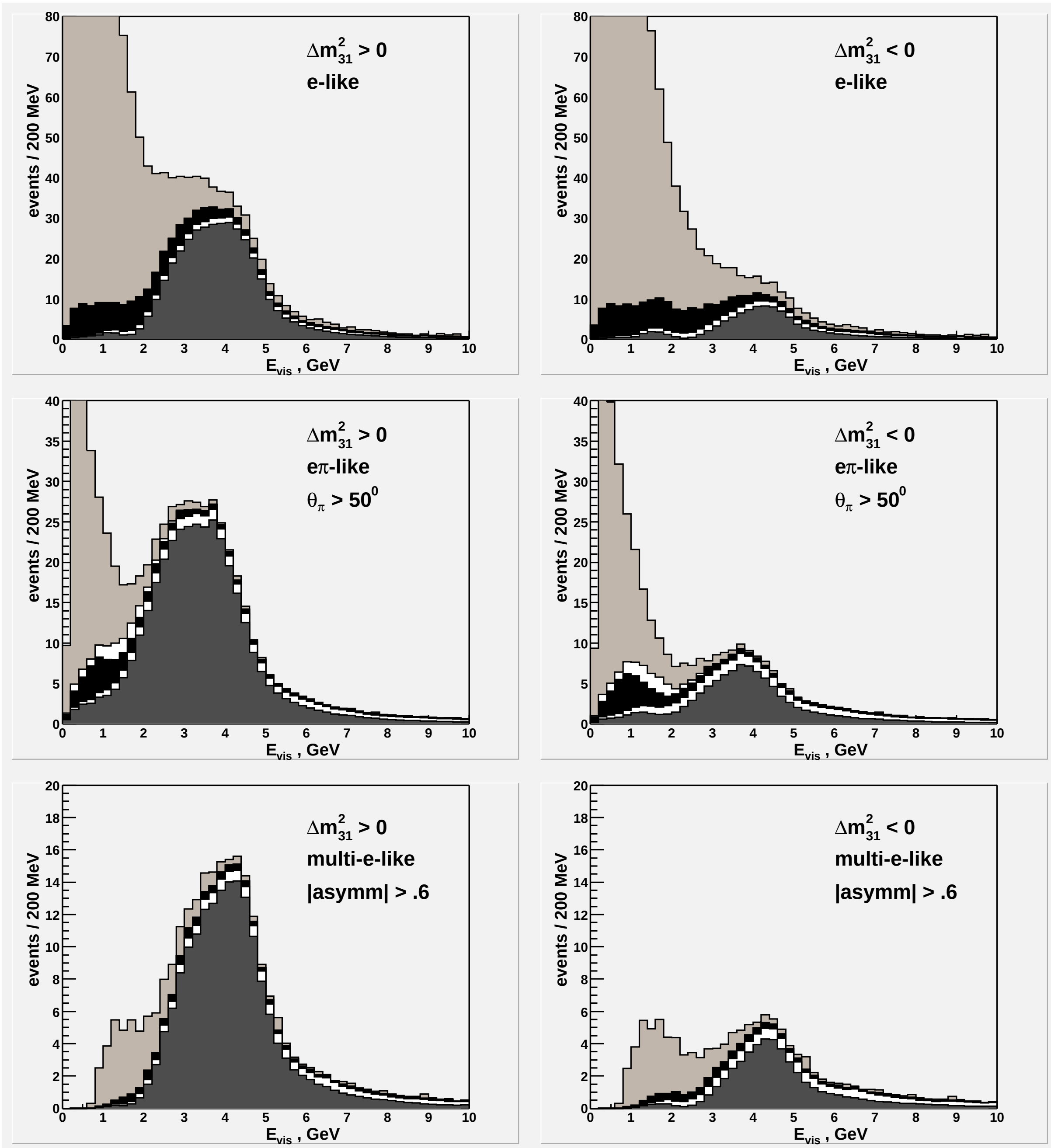

Figure 5: Same as Fig. 3, but for $L = 1770$ km and $\theta_\nu = 5.6$ mrad.

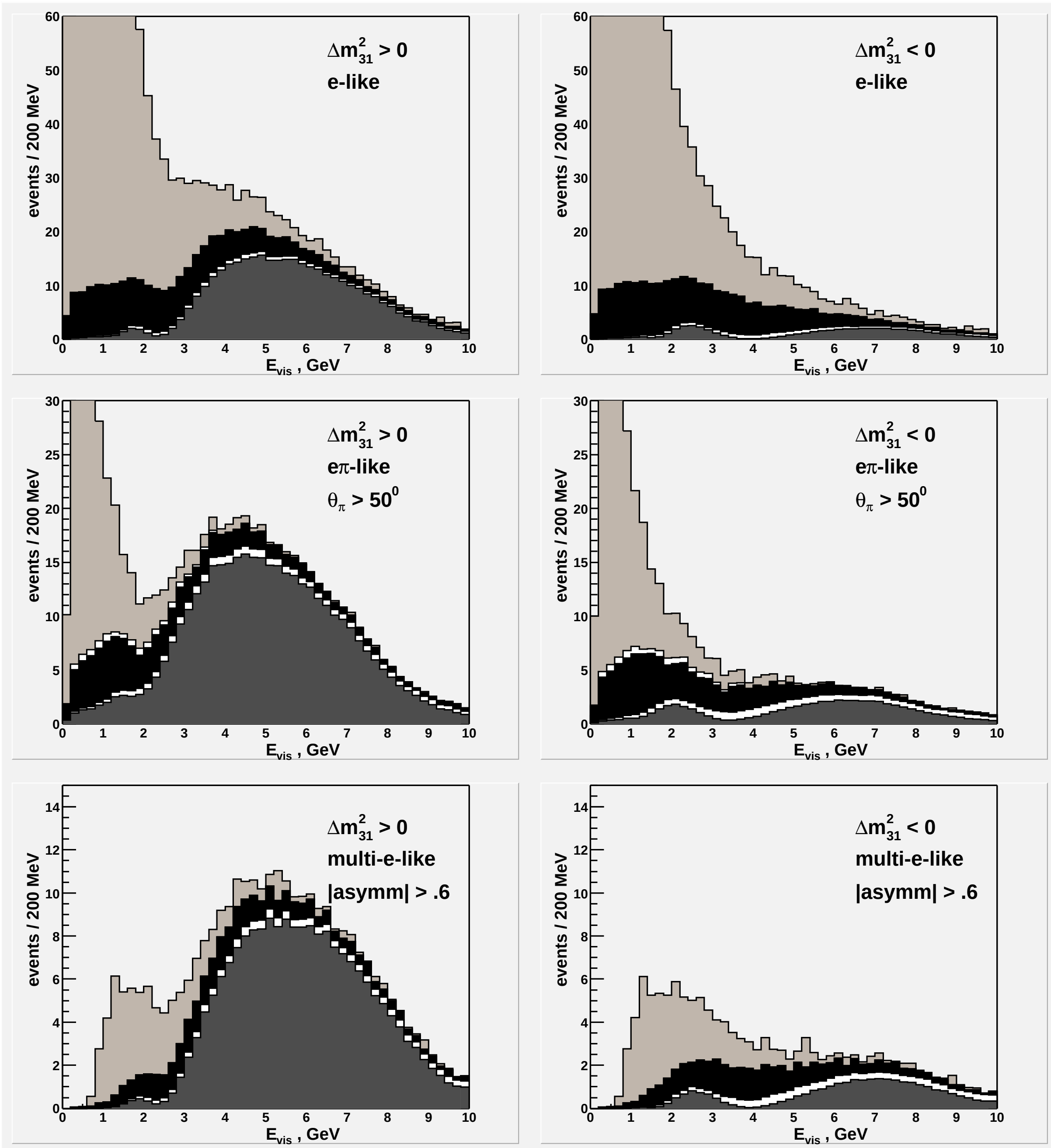

Figure 6: Same as Fig. 3, but for $L = 2620$ km and $\theta_\nu = 0$.